Self-Diffusion in Silicon: Similarity between the Properties of Native Point Defects

Ant Ural,* P. B. Griffin, and J. D. Plummer
Department of Electrical Engineering, Stanford University, Stanford, California 94305
(Received 7 June 1999)

Self-diffusion measurements in silicon are extended to the range 800–900 °C by monitoring ^{30}Si diffusion in isotopically enriched structures. Comparing P, Sb, and self-diffusion under nonequilibrium conditions, we determine that the interstitial-mediated fraction of self-diffusion is confined between 0.50 and 0.62 in the temperature range of 800–1100 °C. This allows activation enthalpies of 4.68 and 4.86 eV to be determined for the interstitial and vacancy mechanisms, respectively. Both mechanisms are also found to exhibit large activation entropies. This result is in contrast to values extracted from metal diffusion experiments.

PACS numbers: 66.30.Hs, 61.72.Ji

Understanding the atomic-scale mechanisms of solid-state diffusion in silicon at elevated temperatures is of broad scientific and technological interest. The most fundamental of such diffusion processes is self-diffusion. Experimental study of self-diffusion is key to unveiling the properties of the native point defects in Si, providing quantitative comparison to theoretical results from the rapidly advancing field of *ab initio* and atomistic calculations. These properties, moreover, serve as key fundamental parameters for predictive modeling of dopant diffusion in state-of-the-art semiconductor device technology.

On the atomic scale, diffusion in silicon can be mediated by either native point defects, namely, self-interstitials (I) and vacancies (V), or by a direct substitutional exchange mechanism (E) which occurs in their absence [1–4]. Despite many years of research, there has been an intense debate about which one of these three mechanisms dominates self-diffusion. Recently, epitaxial growth of isotopically enriched Si structures has been possible, opening the way for direct experimental observation of self-diffusion phenomena for the first time [5,6]. Experiments under thermal equilibrium concentrations of native point defects have shown that the Si self-diffusion coefficient D_{Si}^{eq} exhibits Arrhenius behavior,

$$D(T) = d_0 \exp(-H/k_B T), \qquad (1)$$

with a single activation enthalpy, H, and prefactor d_0 in the temperature range 850–1400 °C [5]. In Eq. (1), T denotes absolute temperature, and k_B is the Boltzmann's constant. In addition, utilizing similar isotope structures, we have recently reported nonequilibrium experiments, where point defect concentrations have been perturbed from their thermal equilibrium values by thermal oxidation and nitridation [6]. These experiments have provided direct evidence that Si self-diffusion is mediated by a dual vacancy-interstitial mechanism with the possibility of a small exchange component.

In this Letter, we investigate self-diffusion in Si at 800 and 900 °C. Combining these results with our data at 1000 and 1100 °C [6] enables us to determine the activation enthalpies of the native point defects in Si. We create nonequilibrium point defect concentrations by thermal oxidation, a well-studied surface reaction which injects interstitials. Measuring the resulting deviations from equilibrium diffusion coefficients for antimony (a vacancy diffuser), phosphorus (an interstitial diffuser), and self-diffusion under identical anneal conditions, we determine the I- and V-mediated fractions of self-diffusion f_{SiI} and f_{SiV}, in the temperature range 800–1100 °C. The temperature dependence of these fractions gives information about the thermodynamic properties of native point defects. Some preliminary results have been reported in a conference proceedings [7]. Our findings, in disagreement with the currently accepted picture that I dominates self-diffusion at high, and V at low temperatures, demonstrate clearly that both mechanisms have comparable contributions over a wide temperature range. This strong competition is a manifestation of the similarity between the thermodynamic properties of these two native point defects in Si.

Three structures were fabricated for this experiment. The first was a Si isotope structure with an n-type background doping of 10^{15} cm^{-3}, grown by chemical vapor deposition (CVD) with a surface layer of approximately 170 nm containing the three stable isotopes of Si in their natural relative abundances, and a buried layer heavily depleted in ^{29}Si and ^{30}Si. For example, ^{30}Si, the isotope used to monitor self-diffusion, was reduced from a natural abundance of 3.10% at the surface to 0.002% at the buried layer. The self-diffusion coefficient has a small dependence on the mass of the diffusing species (the isotope effect), but the difference between the diffusivities of the three isotopes of Si is calculated to be no more than 1%, which is negligible in comparison to the experimental error. The second and third structures grown were P and Sb doped Si, fabricated by ion implantation of the respective species, an inert drive-in anneal at 1100 °C for 5 h, and CVD growth of intrinsic natural Si to form the surface layer for the dopants to diffuse into.

After growth, these three structures were annealed in a furnace in an oxidizing (100% O_2) ambient at 800–1100 °C for times between 1 and 100 h. In addition,

 0031-9007/99/83(17)/3454(4)$15.00

all structures were annealed in an inert ambient (100% Ar) at temperatures ranging from 900 to 1100 °C for times between 1 and 72 h. The equilibrium (inert anneal) diffusivity values at 800 °C were extrapolated from higher temperature data.

The diffusion profiles resulting from all anneals along with the as-grown profiles for ^{30}Si, P, and Sb were obtained by secondary ion mass spectroscopy (SIMS). SIMS analysis for ^{30}Si was performed on a CAMECA-4f instrument with a 3 keV O_2^+ primary beam at an average sputtering rate of 5 Å/s. For P and Sb, a CAMECA-3f instrument with a 14.5 keV Cs^+ beam was used. We have explicitly verified by a convolution routine that values of the extracted self-diffusion coefficients are left unchanged by any possible SIMS broadening effects due to ion beam mixing.

The P, Sb, and self-diffusion coefficients in Si under both inert and oxidizing ambients were extracted by taking the as-grown profile, and using TSUPREM-4, a simulation program, to numerically diffuse it by solving Fick's second law until a match was achieved with the SIMS profile after annealing. The extrinsic conditions in the P and Sb structures cause some slight concentration dependent diffusion, and also set up an internal electric field which results in an additional drift component of diffusion [2]. These effects as well as furnace temperature ramp periods were taken into account in the simulation program. Small correction factors for the depth and concentration scales were also included as parameters in this least-squares fitting process. Figure 1 shows the SIMS profiles for the 24 h inert anneal and 36 h oxidation at 900 °C for the Si isotope structure, along with the corresponding simulation fits. The extracted equilibrium diffusion coefficients show a good fit to Arrhenius behavior [Eq. (1)] with a single activation enthalpy in all cases. For P and Sb, we find that $D_P^{\mathrm{eq}} = 1.37\exp(-3.55/k_BT)$ and $D_{Sb}^{\mathrm{eq}} = 49.0\exp(-4.19/k_BT)$ cm^2/s, respectively. These values agree well with previously published data [8]. In addition, the equilibrium self-diffusion coefficients exhibit an excellent fit to the expression obtained in Ref. [5], $D_{Si}^{\mathrm{eq}} = 560\exp(-4.76/k_BT)$ cm^2/s, and lie well within the error bars reported in that work. The data points and best fits for all three cases are plotted in Fig. 2 as a function of inverse absolute temperature.

The ratio of the diffusivity under oxidation to that under inert annealing for each species is listed in Table I at temperatures of 800–1100 °C. The ratios at 1000 and 1100 °C were taken from our earlier work [6], normalized by the corresponding equilibrium diffusivities obtained in the preceding paragraph [9]. The diffusivity ratios under oxidation are related to the fractional contributions of atomic-scale diffusion mechanisms by [2,10]

$$\frac{D_A^{\mathrm{ox}}}{D_A^{\mathrm{eq}}} = f_{AI}\,\frac{C_I^{\mathrm{ox}}}{C_I^{\mathrm{eq}}} + f_{AV}\,\frac{C_V^{\mathrm{ox}}}{C_V^{\mathrm{eq}}} + f_{AE}\,, \qquad (2)$$

where A represents the diffusing species (A = P, Sb, or in the case of self-diffusion, Si), and f_{AI}, f_{AV}, and f_{AE} are the I, V, and E fractions, respectively, of A diffusion under equilibrium conditions. These fractions are constants at a given temperature. In the case of equilibrium, denoted by the superscript eq, Eq. (2) reduces to the normalization condition, $f_{AI} + f_{AV} + f_{AE} = 1$. For self-diffusion, Eq. (2) is exact; for dopant impurities like P and Sb, it holds true to a very good approximation, as discussed in detail in Ref. [10]. The ratios involving the I and V concentrations, C_I and C_V on the right-hand side, are the perturbation levels of these defects under nonequilibrium conditions. The superscript ox denotes oxidation. Diffusivity ratios and point defect perturbation levels measured at the end of the experiment are time averaged values. Point defects exist in multiple charge states whose properties depend on the Fermi level.

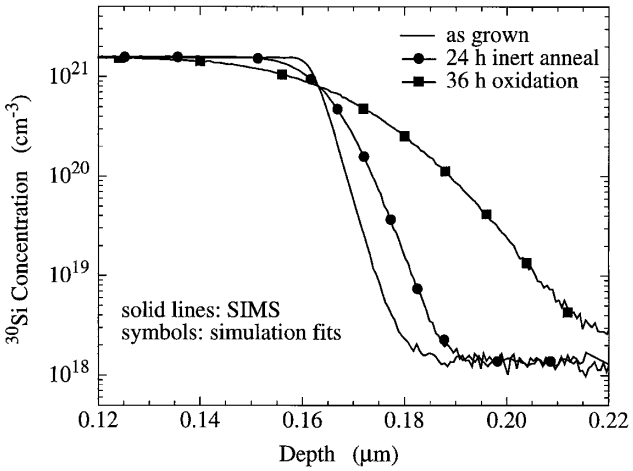

FIG. 1. Diffusion profiles of ^{30}Si in the isotopically enriched structure after 24 h inert anneal and 36 h oxidation at 900 °C. The solid lines are the measured SIMS profiles, whereas the symbols show the simulation fits used for extracting diffusion coefficients. The as-grown profile is also given for reference.

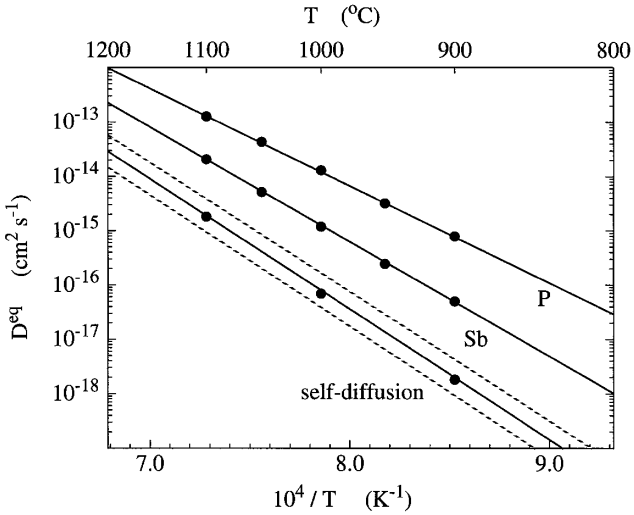

FIG. 2. Arrhenius plots of the equilibrium diffusion coefficients for P, Sb, and self-diffusion in Si. The symbols are the data points, and the solid lines show the best fits given in the text. The two dashed lines represent the lower and upper bounds of experimental error for the self-diffusion coefficient reported in Ref. [5].

TABLE I. Measured diffusivity ratios for ^{30}Si, P, and Sb under oxidation, and f_{SiI} in the temperature range 800–1100 °C. The oxidation times are 1, 5, 36, and 100 h, respectively, at 1100, 1000, 900, and 800 °C.

	Diffusivity ratios under oxidation			
	^{30}Si	P	Sb	f_{SiI}
1100 °C	1.53	2.69	0.349	0.502
1000 °C	2.46	4.09	0.260	0.575
900 °C	5.16	8.39	0.198	0.605
800 °C	14.57	23.60	<0.194	0.614

Since intrinsic carrier concentrations prevail in our isotope structures over the whole temperature range of this study, no disguised temperature dependence is introduced in the calculation of point defect properties. All values reported in this work represent an average over possible charge states present under intrinsic conditions.

It has been well established that, during oxidation, the perturbation of point defects from equilibrium is in the form of interstitial injection from the surface into the bulk, causing a supersaturation of I and an undersaturation of V [2]. It has also been well established from both experiment and theory that P diffusion is mediated almost exclusively by an I mechanism (i.e., $f_{PI} \approx 1$), whereas Sb diffuses predominantly by vacancies ($f_{SbI} \approx 0$) [2,3,10]. Consequently, oxidation results in a P diffusivity enhancement comparable in magnitude to the supersaturation of I, and an Sb retardation equal to the undersaturation of V. Finally, a combination of nitridation and oxidation anneals at 1000 and 1100 °C has concluded that even if there is an E component of Si self-diffusion, its contribution is much smaller than those of the point defect mechanisms [6]. Furthermore, theoretical calculations have predicted the E component to be at least an order of magnitude smaller than I and V components [11].

Assuming $f_{PI} = 1$, $f_{SbI} = 0$, and $f_{SiE} = 0$ based on the discussion in the preceding paragraph, we have solved Eq. (2) for f_{SiI}, and listed the values obtained in the temperature range 800–1100 °C in the last column of Table I. These values are also plotted in Fig. 3, including the error bars. These error bars are due partly to relaxing the above assumptions on f_{PI}, f_{SbI}, and f_{SiE}, and partly to taking into account experimental uncertainty. In recent experiments, we have shown that at 1100 and 1000 °C, $f_{PI} \geq 0.96$ and $f_{SiE} \leq 0.14$, and in conjunction with the oxidation data presented in this work, at 800–1100 °C, $f_{SbI} \leq 0.03$ [6,10]. Solving the system of three equations (one equation each for P, Sb, and self-diffusion) having the form Eq. (2) with these upper and lower bounds, and taking into account our estimate of the experimental error, $\pm 5\%$, in the measured diffusivity ratios listed in Table I, we arrive at the error bars shown in Fig. 3. We find that the contribution of experimental uncertainty to the overall error is larger than that of the assumptions on f_{PI}, f_{SbI}, and f_{SiE}. The main component of this uncertainty comes from SIMS crater depth measurements done by stylus profilometry.

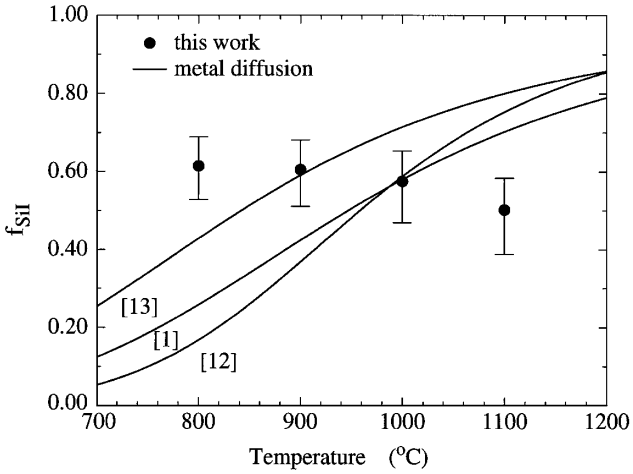

FIG. 3. The I-mediated fraction of self-diffusion f_{SiI} as a function of temperature in the range 800–1100 °C. The symbols show the data points including the error bars. Solid lines are the predictions of metal diffusion experiments where the corresponding reference number is cited in square brackets.

In Fig. 3, we have also plotted, represented by the solid lines, f_{SiI} extracted from experimental studies of substitutional-interstitial metal diffusers (e.g., Au, Zn, and Pt) in Si [1,12,13]. Results from other similar experiments [14], a combination of Zn and self-diffusion data [5], and tight-binding calculations [15] exhibit similar trends. In striking contrast to these results, f_{SiI} obtained directly using isotopically enriched structures manifests a much weaker dependence on temperature. Figure 3 shows that this conclusion is unaltered even if error bars are taken into account. Furthermore, we observe an increase in f_{SiI} with decreasing temperature, which is exactly the opposite of the trend extracted from metal diffusion experiments. By directly monitoring the diffusion of Si atoms, we have avoided some of the assumptions involved in the interpretation of metal diffusion data. Our findings show that within the temperature range 800–1100 °C, f_{SiI} is confined between 0.5 and 0.62.

Ultimately, the temperature dependence of f_{SiI}, and hence f_{SiV}, is closely linked to the thermodynamic properties of the corresponding point defect by

$$f_{SiX}(T) = \frac{d_{0X} \exp(-H_X/k_B T)}{D_{Si}^{\mathrm{eq}}(T)}, \tag{3a}$$

with the temperature independent prefactor given by

$$d_{0X} = l_X g_X a_0^2 \nu_X \exp(S_X/k_B), \tag{3b}$$

where the subscript $X = I$, V, or E, l_X is the correlation factor of order unity (we do not use the traditional notation of f_X for the correlation factor in order to distinguish it from f_{SiX}), g_X is the geometry factor, a_0 is the lattice constant, and ν_X is the attempt frequency. Furthermore, for the point defect mechanisms, the activation enthalpy H_X equals the sum of the formation and migration enthalpies of the defect X, i.e., $H_X = H_X^F + H_X^M$, and similarly, the activation entropy S_X equals the sum of the

respective entropies, i.e., $S_X = S_X^F + S_X^M$. If the activation enthalpies of all diffusion mechanisms were identical, f_{SiX} would be independent of temperature. If, on the other hand, one of the H_X were much smaller than the others, as in the case of P or Sb, $f_{SiX} = 1$ at all temperatures. The weak temperature dependence observed experimentally hints strongly at unequal but comparable activation enthalpies. Equations (3) show clearly that an Arrhenius fit of the X component of self-diffusion D_{SiX}, given by the product of f_{SiX} and D_{Si}^{eq}, yields H_X and S_X. As a result, we find that the I and V components of Si self-diffusion exhibit excellent fit to

$$D_{SiI} = 149 \exp(-4.68/k_B T), \text{ and} \tag{4a}$$

$$D_{SiV} = 636 \exp(-4.86/k_B T)\ \mathrm{cm}^2/\mathrm{s}, \tag{4b}$$

respectively. Using the same values for the constants in Eqs. (3) as in Ref. [5], and taking into account the error bars in our measured results, we get $H_I = 4.68^{+0.12}_{-0.15}$ eV and $H_V = 4.86^{+0.19}_{-0.15}$ eV, and $S_I = 10.2^{+1.2}_{-1.5} k_B$ and $S_V = 12.8^{+1.8}_{-1.5} k_B$. Metal diffusion experiments [1,12–14], a combination of Zn and self-diffusion data [5], tight-binding molecular dynamics calculations [15], and atomistic simulations using the Stillinger-Weber potential [16] predict H_I to be as much as 1 eV larger than H_V. Our results, on the other hand, strongly suggest that the difference between H_I and H_V is on the order of only a few tenths of an eV. The value of H_I obtained in this work agrees, within error bars, with that extracted recently from the energetics of self-interstitial clusters in Si [17]. Focusing on the results for S_I and S_V, we see that both entropies are large and comparable in magnitude. Our results agree with the theoretical findings of Ref. [11] that even simple native point defects can have large entropies of formation, and that S_I^F and S_V^F are similar in magnitude. It is also possible that this large entropy is an indication of the presence of extended defects as proposed previously [18], or of complex defects such as di-vacancies or di-interstitials.

In conclusion, we have studied Si self-diffusion under both equilibrium and nonequilibrium concentrations of point defects using isotopically enriched structures. A comparison of these results with identical anneals for an interstitial diffuser, P, and a vacancy diffuser, Sb, was used to find the temperature dependence of f_{SiI}, and consequently, the thermodynamic properties of the native point defects. These results constitute direct experimental evidence of the strong competition between the I- and V-mediated mechanisms of self-diffusion, and of the astonishing similarity between the energetics of these native point defects in silicon.

We would like to thank S. Burden at Isonics Corporation for providing the enriched ^{28}Si. This work was funded by the Semiconductor Research Corporation.

*Electronic address: antural@leland.stanford.edu

[1] W. Frank, U. Gösele, H. Mehrer, and A. Seeger, in *Diffusion in Crystalline Solids*, edited by G. E. Murch and A. S. Nowick (Academic, New York, 1984), p. 63.

[2] P. M. Fahey, P. B. Griffin, and J. D. Plummer, Rev. Mod. Phys. **61**, 289 (1989).

[3] C. S. Nichols, C. G. Van de Walle, and S. T. Pantelides, Phys. Rev. Lett. **62**, 1049 (1989); Phys. Rev. B **40**, 5484 (1989).

[4] K. C. Pandey, Phys. Rev. Lett. **57**, 2287 (1986); A. Antonelli, S. Ismail-Beigi, E. Kaxiras, and K. C. Pandey, Phys. Rev. B **53**, 1310 (1996).

[5] H. Bracht, E. E. Haller, and R. Clark-Phelps, Phys. Rev. Lett. **81**, 393 (1998); H. Bracht, E. E. Haller, K. Eberl, M. Cardona, and R. Clark-Phelps, in *Diffusion Mechanisms in Crystalline Materials*, edited by Y. Mishin, G. Vogl, N. Cowern, R. Catlow, and D. Farkas (Materials Research Society, Warrendale, PA, 1998), Vol. 527, p. 335.

[6] A. Ural, P. B. Griffin, and J. D. Plummer, Appl. Phys. Lett. **73**, 1706 (1998).

[7] Ant Ural, Peter B. Griffin, and James D. Plummer, Mater. Res. Soc. Symp. Proc. (to be published).

[8] R. B. Fair, in *Impurity Doping Processes in Silicon*, edited by F. F. Y. Wang (North-Holland, Amsterdam, The Netherlands, 1981), p. 315.

[9] The diffusivity ratios at 1000 and 1100 °C given in Table I differ as much as 10% from those previously reported in Ref. [6]. In Ref. [6], the actual equilibrium diffusion coefficients measured at each temperature were used to normalize the corresponding diffusivity under oxidation. Here, we have used the equilibrium diffusivities obtained from Arrhenius best fits of the data over the whole temperature range for normalization. This averaging over data points should help minimize the experimental error.

[10] Ant Ural, Peter B. Griffin, and James D. Plummer, J. Appl. Phys. **85**, 6440 (1999).

[11] P. E. Blöchl, E. Smargiassi, R. Car, D. B. Laks, W. Andreoni, and S. T. Pantelides, Phys. Rev. Lett. **70**, 2435 (1993).

[12] H. Bracht, N. A. Stolwijk, and H. Mehrer, Phys. Rev. B **52**, 16 542 (1995).

[13] H. Bracht, in *Proceedings of the Electrochemical Society Meeting* (The Electrochemical Society, Pennington, NJ, 1999), Vol. 99-1, p. 357; A. Giese, H. Bracht, N. A. Stolwijk, and J. T. Walton, J. Appl. Phys. **83**, 8062 (1998).

[14] See the references in [1,12,13].

[15] M. Tang, L. Colombo, J. Zhu, and T. Diaz de la Rubia, Phys. Rev. B **55**, 14 279 (1997).

[16] D. Maroudas and R. A. Brown, Phys. Rev. B **47**, 15 562 (1993); Appl. Phys. Lett. **62**, 172 (1993).

[17] N. E. B. Cowern, G. Mannino, P. A. Stolk, F. Roozeboom, H. G. A. Huizing, J. G. M. van Berkum, F. Cristiano, A. Claverie, and M. Jaraiz, Phys. Rev. Lett. **82**, 4460 (1999).

[18] A. Seeger and K. P. Chik, Phys. Status Solidi **29**, 455 (1968).